www.sciencemag.org/cgi/content/full/science.1229180/DC1

Supplementary Materials for

Dynamic Topography Change of the Eastern United States Since 3 Million Years Ago

David B. Rowley,* Alessandro M. Forte, Robert Moucha, Jerry X. Mitrovica, Nathan A. Simmons, Stephen P. Grand

*Corresponding author. E-mail: drowley@uchicago.edu

Published 5 July 2013 on *Science* Express
DOI: 10.1126/science.1229180

This PDF file includes:

Materials and Methods
Supplementary Text
Figs. S1 to S6
References

Other Supplementary Material for this manuscript includes the following:
available at www.sciencemag.org/cgi/content/full/science.1229180/DC1

Table S1

Supplementary Text

Retrodiction of Paleogeography

Retrodiction of the paleogeography requires knowledge of the full suite of contributors that have impacted surface elevations between the Present and any time in the past. These would include, but are probably not limited to, thermal subsidence, sediment loading, flexural loading, erosion-related flexural unloading, dissolution of carbonates or salts, together with glacial isostatic adjustment and changes in dynamic topography that were incorporated in Figure 3 of the main text. In this Supplement, we provide estimates of the contributions associated with flexural loading and unloading, present dynamic topography estimates related to combinations of the joint seismic-geodynamic tomography inversions and viscosity models V1 and V2 (see below), and GIA. We judge the uncertainties associated with the flexural calculations to be sufficiently large to not warrant incorporating them in our current retrodictions of the paleogeography.

Dynamic Topography Change Since 3Ma

Four different estimates of dynamic topography change are presented in Figure S1. These represent the combinations of two joint seismic-geodynamic tomography inversions, the 3-D mantle models TX2007 (33) and TX2008 (34), and two different models of viscosity with depth (10, 32), labeled V1 and V2 in the main text. These fields are overlain on the ETOPO1-derived topography of the mid-Pliocene marine flooding surface together with the location of the Orangeburg, Trail Ridge (TR), Chippenham (CS), and Thornburg (TS) Scarps, and the Fall Zone. Note that all four estimates place a maximum uplift in the vicinity of Chesapeake Bay where the surface is most intensely incised. The total changes in dynamic topography (Figure S1) are characterized by a fundamentally non-linear spatio-temporal evolution that results from the combined non-linearity of the time-dependence of 3-D buoyancy in the mantle and the "advection" of the topography signal due to horizontal motion of the overlying North American plate. Type or paste text here. This should be additional explanatory text, such as: extended technical descriptions of results, full details of mathematical models, extended lists of acknowledgements etc. It should not be additional discussion, analysis, interpretation or critique. Keep this formatting or style as SM text.

Importance of hot, buoyant mantle under the eastern US

The dynamical importance of hot buoyant material under the eastern U.S. was first made evident in previous calculations (15) that focused on the impact of Farallon subduction under the central US, where shallow-angle upwelling mantle under the east coast resembles 'corner flow' above the subducting slab (see also Figure S2). However, we emphasize that this does not appear to be passive return flow, because we find a source of deep buoyancy under the Atlantic mantle adjacent to the US coastal margin that extends to the Bermuda swell (see Figure 4a in Ref. (15)). As we next demonstrate, this westward transport of upper-mantle buoyancy under the eastern U.S. (Figure S2) is an important contributor to the dynamic topography.

To elucidate the dynamical importance of upper-mantle buoyancy for the evolution of east coast topography, we calculated the present-day dynamic topography due only to hotter-than-average material in the upper mantle under the Atlantic Ocean (Figure S3).

The mantle 'swell' due to buoyancy that is centered under Bermuda extends a considerable distance westward, towards the eastern margin of the US. This hot, buoyant material is being advected westwards (and upwards) by the prevailing mantle circulation (Figure S2). As a consequence, there will be a progressive 'wave' of topographic uplift, associated with the westward transport of the topography signal in Figure S3, that produces the variable post-Pliocene uplift shown in Figures S1a-d.

Retrodicted Paleogeography at 3 Ma

The four different estimates of dynamic topography change presented in Figure S1 together with the GIA correction shown in Figure 1 of the main text yield four estimates of the paleogeography of the eastern seaboard at 3 Ma, with an additional parameter being the height of sea level at 3 Ma relative to Present. Figure S4a shows the retrodicted paleogeography applying only the TX2008 and V2 dynamic topography correction without any GIA correction and sea level set at +25m, while Figure S4b shows the same but only applying the V2 GIA correction without any dynamic topography correction and with sea level set at +25m. Figure S4c-j shows the retrodicted paleogeography for each of the 4 combinations of model parameters considered in Figure S1 and for two different bounds on the height of mid-Pliocene sea level. Figures S4c-f place this sea level at +25m relative to present and Figures S4g-j place it at 0m. These images show that for much of this region there is a reasonably close spatial correlation between the retrodicted paleogeography and observations, irrespective of the specific combination of tomography and viscosity. Along most of the eastern seaboard, a height of the mid-Pliocene marine highstand somewhere between 0 and +25 m matches the position of the Orangeburg and correlative shoreline-related scarps as well as known locations of marine mid-Pliocene sedimentary rocks. However, the current spatial resolution of the dynamic topography models, as well as uncertainties in other processes contributing to the topography, which we discuss below, suggest that it would be premature to consider this range to be a robust bound on mid-Pliocene sea level.

3-D lithospheric flexure modeling

There is a substantial volume of sediment in offshore basins along the Atlantic and Gulf coasts of North America (16-18). Much of this sediment is either Triassic/Jurassic or Middle Miocene and younger in age (17, 18, 42). This load, and specifically the Neogene sediments, would be expected to have warped the Coastal Plain surface, resulting in uplift of the surface inland, and thus likely perturbed the elevation of Pliocene and younger shorelines (7). We used isopach maps for the entire Neogene (17) to compute the flexural response (Figure S5). We currently lack more detailed isopach maps of just the Pliocene and younger sequences along the entire Atlantic and Gulf coast margins that would be needed to estimate the impact of flexural loading over the entire area of interest.

We modulate the total Neogene flexural loading by ascribing ~30% of total loading to effects associated with Pliocene (at 5.0 Ma) and younger sediment loads, based on data from the Baltimore Canyon Trough where better stratigraphic resolution allows the distinction between Miocene and post-Miocene sequences (18, 42). We assumed a constant rate of sediment-related loading since the Miocene resulting in a 6%/m.y. change in the total sediment load since 5 Ma, in accord with available data (42).

The 3-D flexural response to the offshore sediment load for the entire region from George’s Bank off Nova Scotia to all of the Gulf of Mexico is computed in order to capture longer wavelength contributions from regions outside our main area of interest. This response is calculated by expanding the sediment thickness into spherical harmonics up to harmonic degree and order 360 (corresponding to a resolution scale - half-wavelength - of about 0.5°). A Lanczos-smoothing of this harmonic expansion was applied to mute the Gibbs oscillations ('ringing') associated with this truncated representation. The flexure calculation adopts parameters from the 2-D study of Pazzaglia & Gardner (7), which are based on a 40-km thick elastic plate with a Young's modulus of 70 GPa. The calculation used a sediment density of 2000 kg/m^3, mantle/lithosphere density of 3200 kg/m^3, and water density of 1000 kg/m^3. The effective submarine 'load'-density sitting on the elastic plate is the difference between the sediments and water density and hence is equal to 1000 kg/m^3.

Erosional unloading (see (7)) should also be considered; however, the amplitude and distribution of erosion since 5 Ma is extremely poorly known. Local estimates (43-45) typically average about 20 m/Ma, but range from 0.6 to 57 m/Ma. For the present analysis we used a modified version of a post-50 Ma estimate of erosion rates (46). We suspect that these are maximum estimates (46). There is considerable uncertainty in the estimate of the spatial pattern of erosion because the number of locations with sufficient data is limited and the techniques used to derive the local estimates have their own uncertainties or are varied. The 3-D flexural response to erosional unloading follows the same procedure as above, except that the density of the unloaded material is 2700 kg/m^3. On this basis, we estimate the amplitude of combined sediment load-related flexure and erosion-related flexural unloading as +20m to -8m along the Orangeburg Scarp (Figure S5.

Glacial Isostatic Adjustment

Our numerical predictions of GIA follow the methodology outlined in detail in Ref. (28). These calculations require, as input, the space-time history of ice cover since 3 Ma, and a radial profile of mantle viscosity. In regard to the former, predictions of the contribution from GIA to the current elevation of mid-Pliocene shorelines are most sensitive to the ice history over the last glacial cycle, and we adopt, for this purpose, the ICE-5G model (47).

In Figure S6 we show the topographic perturbation due to GIA along the Orangeburg Scarp, from 55°-59.5° colatitude, computed using six different mantle viscosity profiles, including the V2 model (solid blue line) adopted in Figures 1 and 3 of the main text and Figure S4. Model V2 was derived from a joint inversion of data related to both mantle convective flow and GIA observables, where the latter included post-glacial decay times from Hudson Bay and Fennoscandia, and it is characterized by a viscosity that increases two orders of magnitude with depth in the lower mantle before decreasing near the core-mantle-boundary (10). Model VM2 (47) is based on GIA data alone, and it is defined by a lower mantle viscosity that increases by a factor of only 2-3 with depth. The calculation adopting this model (dashed blue line) predicts a GIA contribution to the topography that is less than 5m, and a mean perturbation that is ~10m less than predicted using model V2.

Neither model V2 nor VM2 are tuned to fit GIA data sets along the US east coast. Indeed, GIA predictions based on the VM2 viscosity profile are known to significantly misfit Holocene relative sea-level curves along this coast (48). Since neither model is likely representative of the viscosity profile beneath the east coast, we also show results generated using four viscosity profiles distinguished on the basis of the adopted (and assumed constant) lower mantle viscosity (red lines), which ranges from $3\text{-}20\times10^{21}$ Pa s. This range brackets nearly all previous inferences of mean lower mantle viscosity based on GIA data. The associated predictions show little geographic variability along the Orangeburg Scarp. However, increasing the mantle viscosity from the lower to upper end of the viscosity range significantly increases the mean topographic perturbation due to GIA from 6m to 27m. We note that a study of tide gauge records along the US east coast demonstrated that the geographic variation in ongoing sea-level rates along this coast was best fit for models with a lower mantle viscosity greater than 5×10^{21} Pa s (49). For this class of models, the mean perturbation due to GIA exceeds 15 m. In any case, the wide range of predictions generated using the 6 viscosity profiles indicates that uncertainties in the GIA contribution complicate any effort to infer mid-Pliocene sea level relative to present (*16*), even without the additional uncertainties associated with dynamic topography or sediment redistribution.

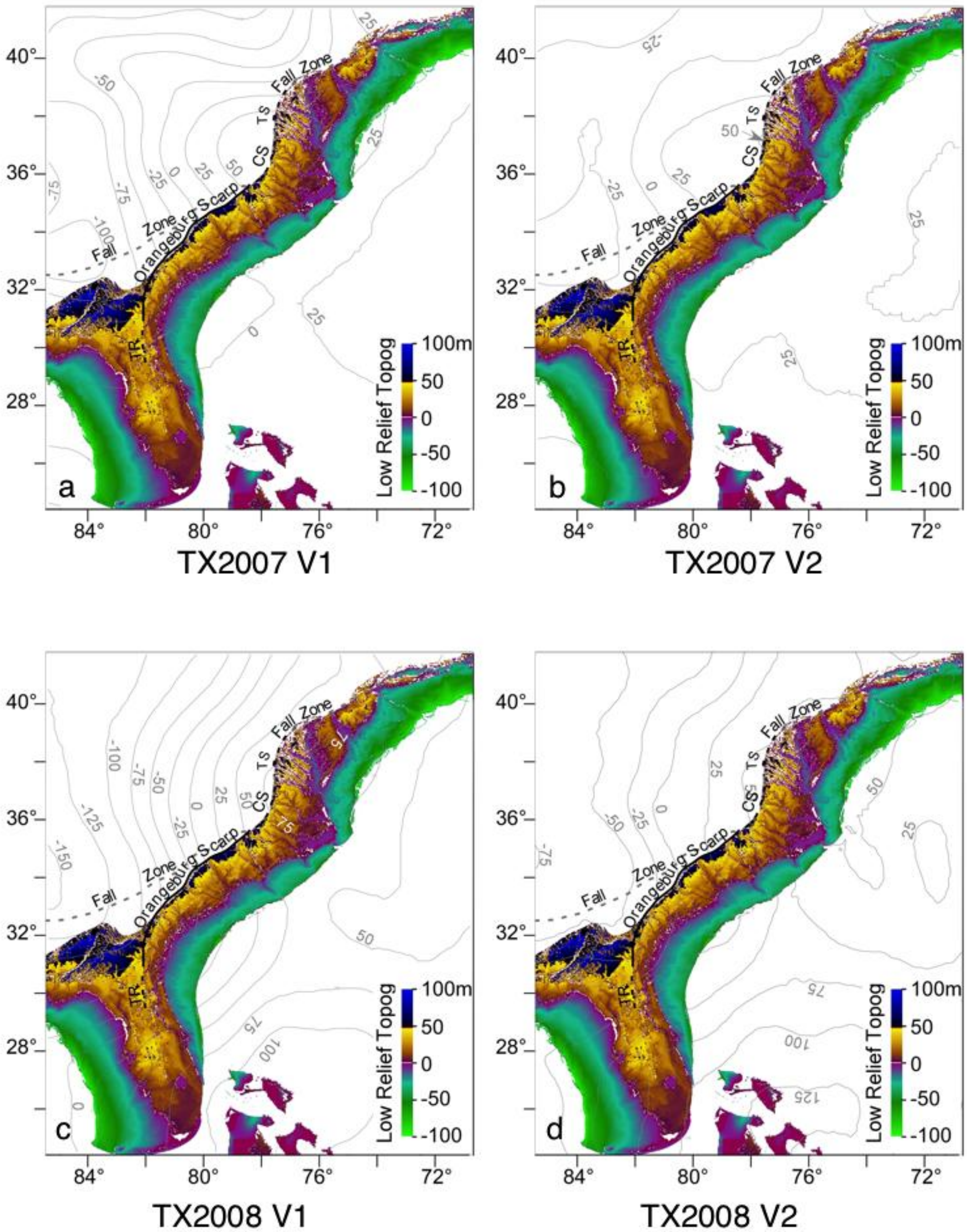

Fig. S1.

Fig. S1. Estimates of dynamic topography change since 3 Ma based on two different joint seismic-geodynamic tomography inversions and two different viscosity profiles (as labeled; see text). Contour interval is 25 m and values are placed on the up-slope side of the contours.

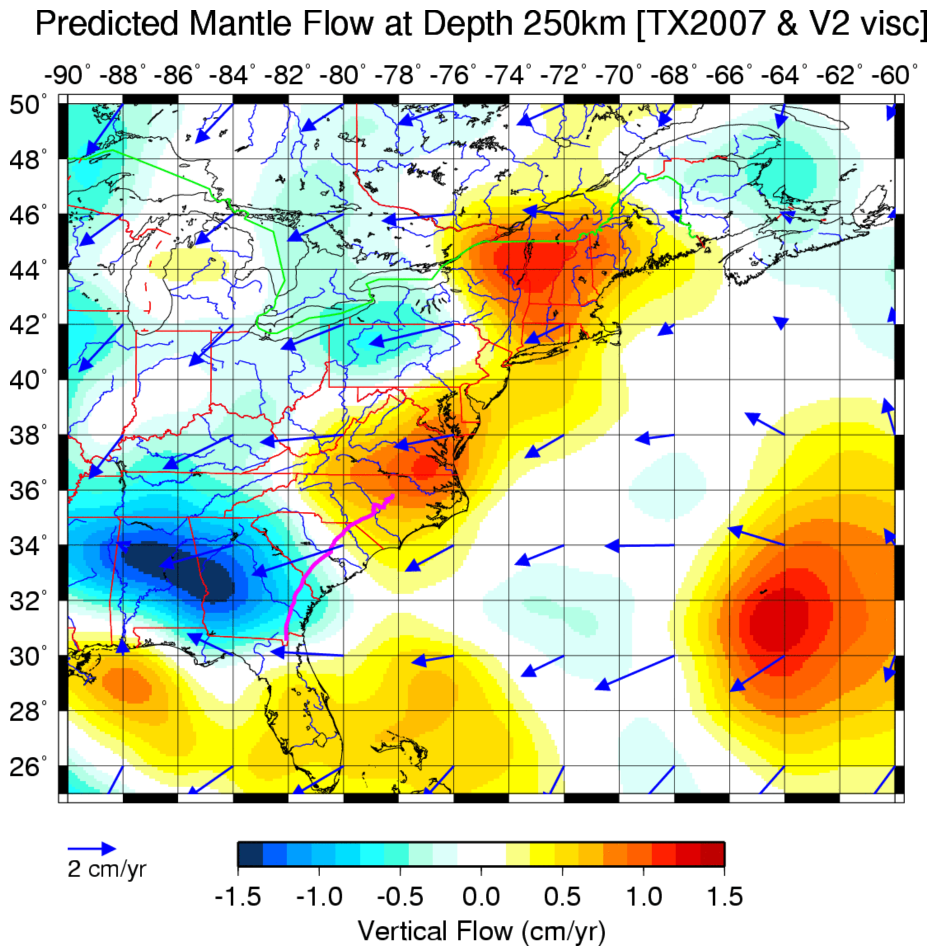

Fig. S2

Fig. S2. Present-day mantle convective flow in the asthenosphere (250 km depth) under the east coast of the United States and adjacent Atlantic Ocean. The flow is predicted using the TX2007 joint seismic-geodynamic tomography model (33) and the V2 viscosity model (31, 32). The color contours (scale bar at bottom center) represent the vertical component of the flow and the blue arrows (scale at bottom left) the horizontal component. The mantle flow is represented in terms of a spherical harmonic expansion up to degree 128

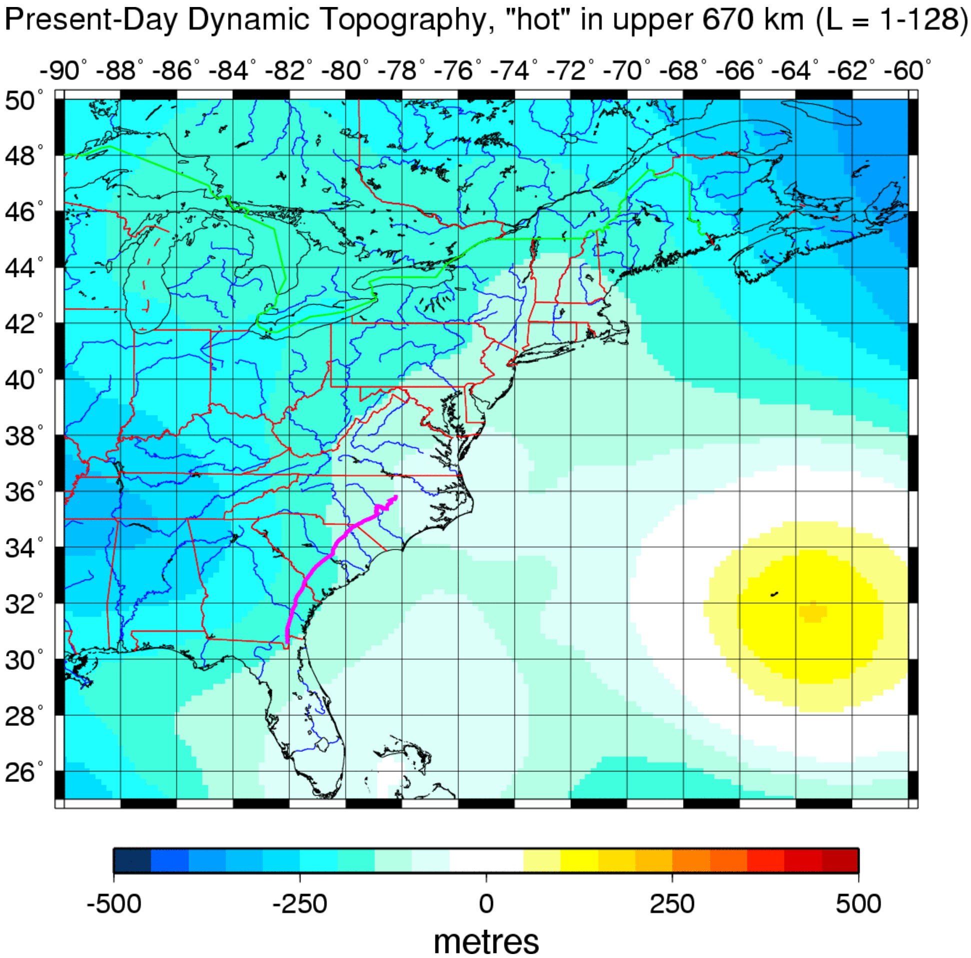

Fig. S3

Fig. S3. Present-day dynamic topography due only to hot, buoyant material in the upper mantle. This prediction is obtained in a mantle flow calculation in which we strip away (zero out) all 'cold' heterogeneity (characterized by faster than average shear-wave velocity) in the joint seismic-geodynamic tomography model TX2007 (33) and by using only the residual 'hot' heterogeneity in the upper mantle (down to 670 km depth). The V2 viscosity model (31) is used in this calculation. The color contours (scale bar at bottom) represent the vertical surface deflection. The mantle flow is represented in terms of a spherical harmonic expansion up to degree 128.

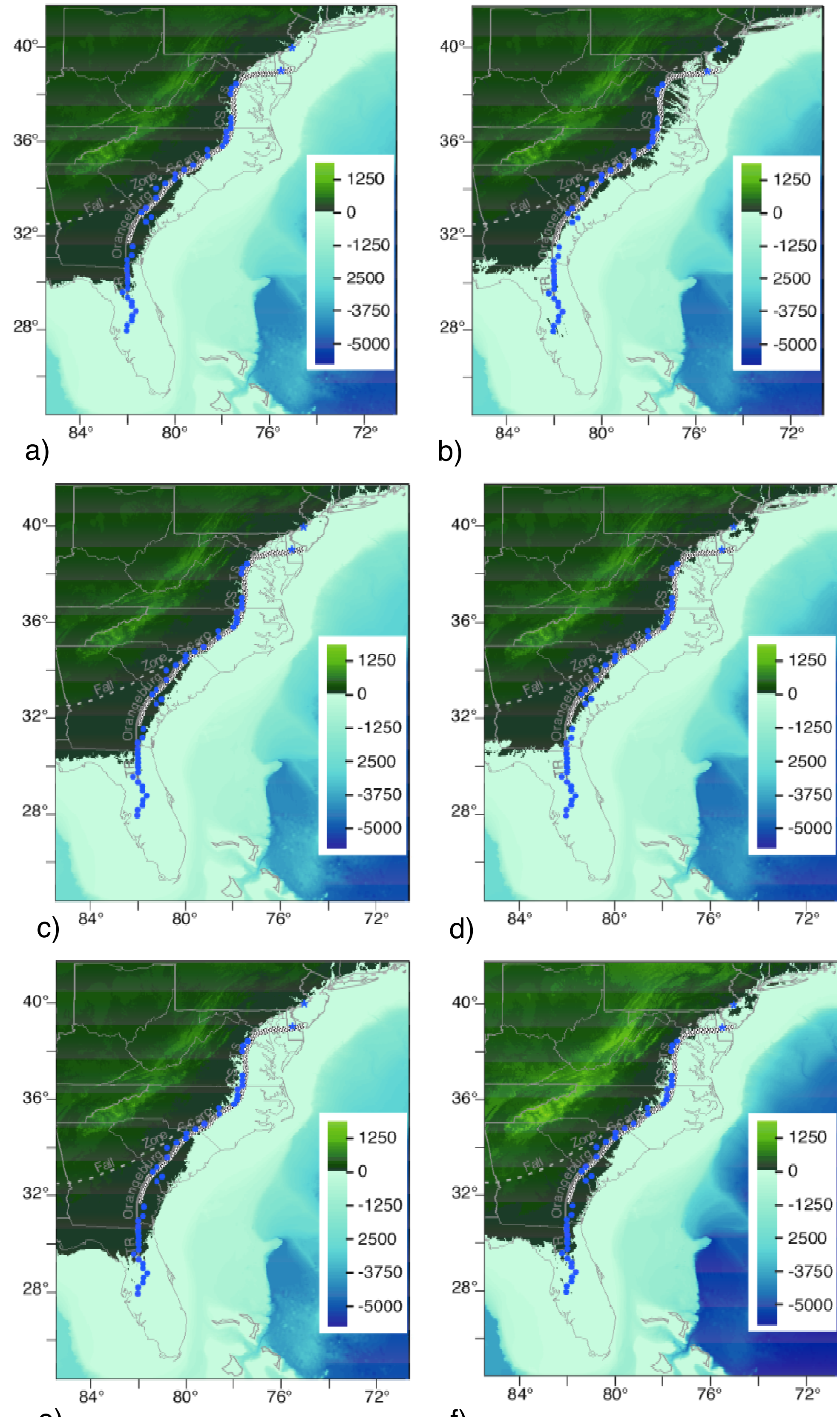

40°
36°
32°
28°
84°
80°
76°
72°
1250
0
-1250
2500
-3750
-5000
Fall
Zone
Orangeburg
Scarp
TR
CS
TS
a)
b)
c)
d)
e)
f)

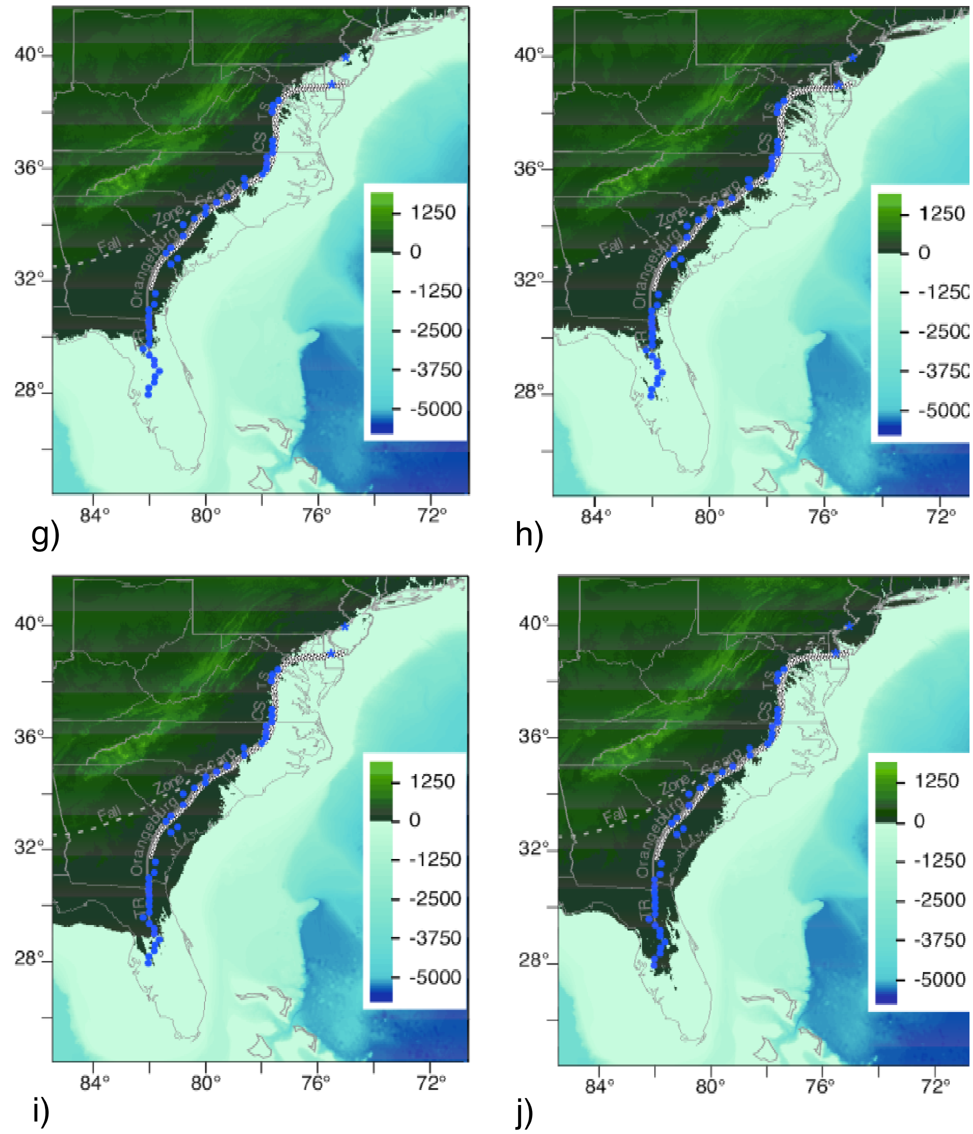

Fig. S4. Retrodicted paleogeographic maps applying (a) TX2008 and V2 with shoreline placed at +25m but without any GIA correction, (b) only the V2 GIA correction, (c) TX2008 and V2 with shoreline placed at +25m but without any GIA correction, (d) TX2007 and V2 with shoreline placed at +25m, (e) TX2008 and V1 with shoreline placed at +25m, (f) TX2007 and V1 with shoreline placed at +25m, (g-j) analogous to frames (c-f), except that the shoreline is placed at 0m.

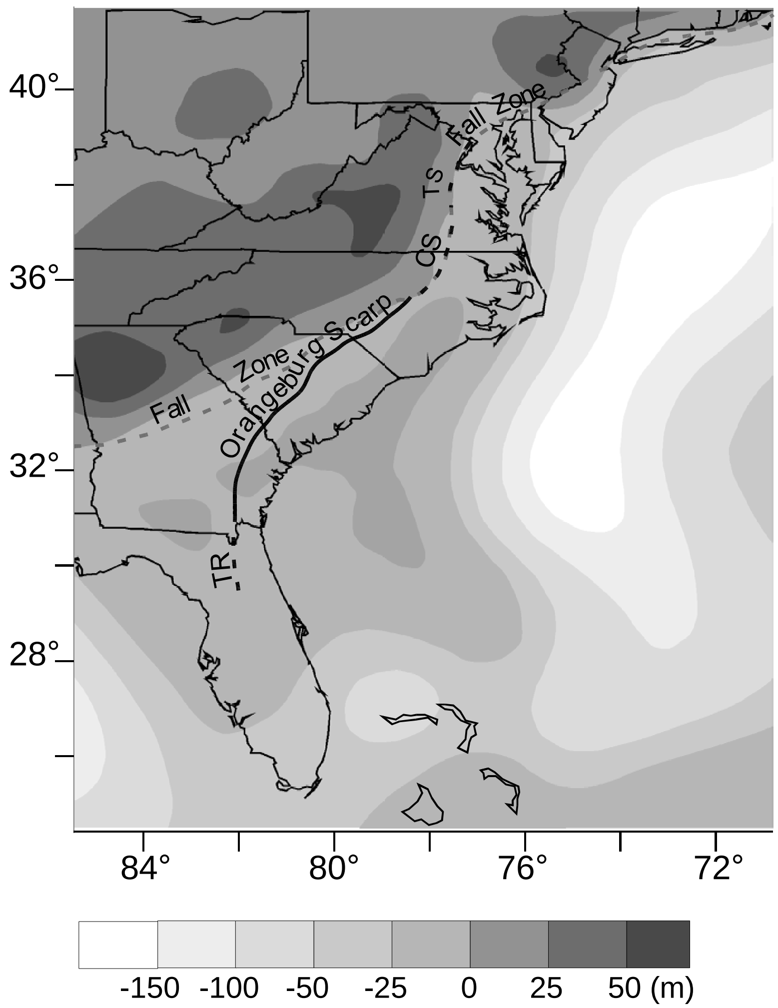

Fig. S5. Estimate of the 3D flexural response associated with sediment-loading and erosional unloading since 3 Ma. Abbreviations are the same as in Figure S1.

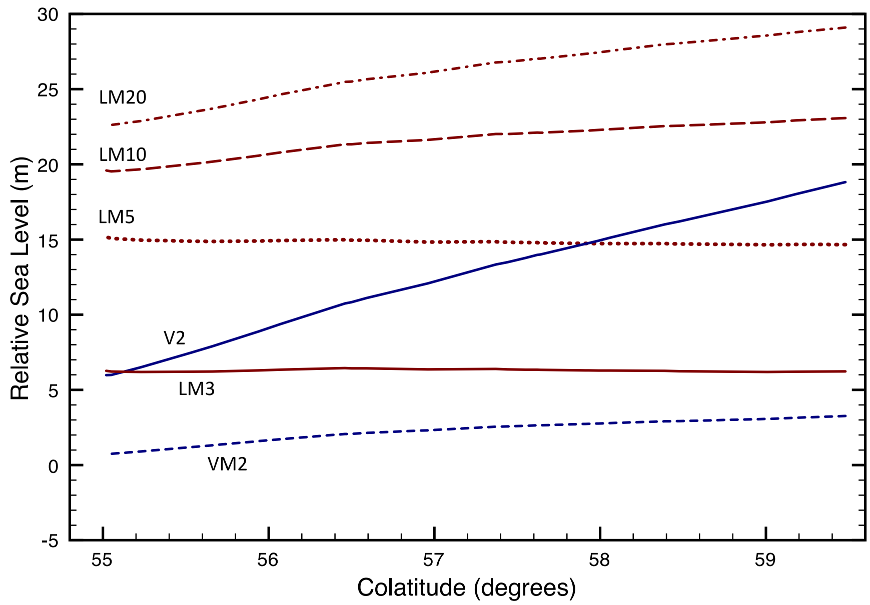

Fig. S6. Predictions of the present-day topographic perturbation along the Orangeburg Scarp due to GIA. The results are generated using the ice history described in Ref. (*15*) and six different profiles of mantle viscosity. These are: models V2 (10), VM2 (47), and four models characterized by constant lower mantle viscosities of 3×10^{21} Pa s (LM3), 5×10^{21} Pa s (LM5), 10^{22} Pa s (LM10) and 2×10^{22} Pa s (LM20). The latter four models are also characterized by an elastic lithosphere of thickness 96 km and an upper mantle viscosity of 5×10^{20} Pa s.

Table S1. Topography, dynamic topography changes, glacial isostatic adjustment, and estimates of flexural loading and unloading corrections for the eastern U.S. for 3Ma to present at 0.2° by 0.2° resolution. Topography derived from regridding of ETOPO1. All values are in meters. See associated discussion in the supplemental text for sources.

References and Notes

1. C. L. Drake, M. Ewing, G. H. Sutton, in *Physics and chemistry of the earth*. (Pergamon Press, Elmsford NY, 1959), vol. 3, pp. 110-198.

2. D. McKenzie, Some Remarks On Development Of Sedimentary Basins. *Earth Planet. Sci. Lett.* **40**, 25 (1978). doi:10.1016/0012-821X(78)90071-7

3. J. V. Browning *et al*., 100 Myr record of sequences, sedimentary facies and sea level change from Ocean Drilling Program onshore coreholes, US Mid-Atlantic coastal plain. *Basin Res.* **20**, 227 (2008). doi:10.1111/j.1365-2117.2008.00360.x

4. M. A. Kominz *et al*., Late Cretaceous to Miocene sea-level estimates from the New Jersey and Delaware coastal plain coreholes: an error analysis. *Basin Res.* **20**, 211 (2008). doi:10.1111/j.1365-2117.2008.00354.x

5. A. B. Watts, M. S. Steckler, in *Deep drilling results in the Atlantic Ocean; continental margins and paleoenvironment,* M. Talwani, W. Hay, W. B. F. Ryan, Eds. (American Geophysical Union, Washington, D.C., 1979), vol. 3, pp. 218-234.

6. A. B. Watts, J. Thorne, Tectonics, global changes in sea level and their relationship to stratigraphical sequences at the US Atlantic continental margin. *Mar. Pet. Geol.* **1**, 319 (1984). doi:10.1016/0264-8172(84)90134-X

7. F. Pazzaglia, T. Gardner, Late Cenozoic flexural deformation of the middle U.S. Atlantic passive margin. *J. Geophys. Res.* **99**, 12143 (1994). doi:10.1029/93JB03130

8. H. J. Dowsett, T. Cronin, High eustatic sea level during the middle Pliocene: Evidence from the southeastern U.S. Atlantic Coastal Plain. *Geology* **18**, 435 (1990). doi:10.1130/0091-7613(1990)018<0435:HESLDT>2.3.CO;2

9. K. G. Miller *et al*., The Phanerozoic record of global sea-level change. *Science* **310**, 1293 (2005). doi:10.1126/science.1116412 Medline

10. R. Moucha *et al*., Dynamic topography and long-term sea-level variations: There is no such thing as a stable continental platform. *Earth Planet. Sci. Lett.* **271**, 101 (2008). doi:10.1016/j.epsl.2008.03.056

11. C. P. Conrad, C. Lithgow-Bertelloni, K. E. Louden, Iceland, the Farallon slab, and dynamic topography of the North Atlantic. *Geology* **32**, 177 (2004). doi:10.1130/G20137.1

12. R. Moucha, A. M. Forte, S. Quéré, J. X. Mitrovica, D. B. Rowley, Implications of Mantle Convection for Present-day Rates of Global Sea Level Change. *EOS Transactions Americasn Geophysical Union, Fall Meet. Supplement* **87**, T53D (2006).

13. R. D. Müller, M. Sdrolias, C. Gaina, B. Steinberger, C. Heine, Long-term sea-level fluctuations driven by ocean basin dynamics. *Science* **319**, 1357 (2008). doi:10.1126/science.1151540 Medline

14. S. Spasojević, L. Liu, M. Gurnis, R. D. Müller, The case for dynamic subsidence of the U.S. east coast since the Eocene. *Geophys. Res. Lett.* **35**, 6 (2008). doi:10.1029/2008GL033511

15. A. M. Forte, J. X. Mitrovica, R. Moucha, N. A. Simmons, S. P. Grand, Descent of the ancient Farallon slab drives localized mantle flow below the New Madrid seismic zone. *Geophys. Res. Lett.* **34**, 5 (2007). doi:10.1029/2006GL027895

16. W. Dillon, P. Popenoe, *The Blake Plateau basin and Carolina Trough The Atlantic continental margin; U.S.* R. Sheridan, J. Grow, Eds., (Geol. Soc. Am., Boulder, CO, United States (USA), United States (USA), 1988), pp. 291-328.

17. K. O. Emery, E. Uchupi, *The Geology of the Atlantic Ocean*. (Springer-Verlag, New York, 1984), pp. 1050.

18. C. Poag, W. Sevon, A Record of Appalachian Denudation in Postrift Mesozoic and Cenozoic Sedimentary Deposits of the U.S. Middle Atlantic Continental Margin. *Geomorphology* **2**, 119 (1989). doi:10.1016/0169-555X(89)90009-3

19. L. J. Poppe, P. Popenoe, C. W. Poag, B. A. Swift, Stratigraphic and paleoenvironmental summary of the south-east Georgia embayment: a correlation of exploratory wells. *Mar. Pet. Geol.* **12**, 677 (1995). doi:10.1016/0264-8172(95)98092-J

20. N. H. Sleep, Thermal effects of the formation of Atlantic continental margins by continental breakup. *Geophys. J. Int.* **24**, 325 (1971). doi:10.1111/j.1365-246X.1971.tb02182.x

21. K. G. Miller, Sea Level Change, Last 250 Million Years. in *Encyclopedia of Paleoclimatology and Ancient Environments*, V. Gornitz, Ed. (Springer, Berlin, 2008), pp. 879–893.

22. D. A. Soller, *Geologic and tectonic history of the lower Cape Fear valley, southeastern North Carolina*. U.S. Geological Survey Professional Paper (U.S. Geological Survey, 1988), vol. 1466-A, pp. 60.

23. H. Dowsett *et al*., The PRISM3D paleoenvironmental reconstruction. *Stratigraphy* **7**, 123 (2010).

24. D. Fox, Paleoclimate. Could East Antarctica be headed for big melt? *Science* **328**, 1630 (2010). doi:10.1126/science.328.5986.1630 Medline

25. D. J. Hill, A. M. Haywood, R. C. A. Hindmarsh, P. J. Valdes, *Characterizing ice sheets during the Pliocene: evidence from data and models*. M. Williams, A. M. Haywood, F. J. Gregory, D. N. Schmidt, Eds., Deep-Time Perspectives on Climate Change: Marrying the Signal from Computer Models and Biological Proxies (Geological Soc Publishing House, Bath, 2007), pp. 517-538.

26. C. Winker, J. Howard, Correlation of tectonically deformed shorelines on the southern Atlantic coastal plain. *Geology* **5**, 123 (1977). doi:10.1130/0091-7613(1977)5<123:COTDSO>2.0.CO;2

27. D. Krantz, A Chronology Of Pliocene Sea-Level Fluctuations: The U.S. Middle Atlantic Coastal Plain Record. *Quat. Sci. Rev.* **10**, 163 (1991). doi:10.1016/0277-3791(91)90016-N

28. M. E. Raymo, J. X. Mitrovica, M. J. O'leary, R. M. Deconto, P. J. Hearty, Departures from eustasy in Pliocene sea-level records. *Nat. Geosci.* **4**, 328 (2011). doi:10.1038/ngeo1118

29. P. Adams, N. Opdyke, J. Jaeger, Isostatic uplift driven by karstification and sea-level oscillation: Modeling landscape evolution in north Florida. *Geology* **38**, 531 (2010). doi:10.1130/G30592.1

30. F. Pazzaglia, T. Gardner, M. Summerfield, Ed., (John Wiley & Sons, Chichester, United Kingdom (GBR), United Kingdom (GBR), 2000), pp. 283-302.

31. A. M. Forte *et al*., Joint seismic–geodynamic-mineral physical modelling of African geodynamics: A reconciliation of deep-mantle convection with surface geophysical constraints. *Earth Planet. Sci. Lett.* **295**, 329 (2010). doi:10.1016/j.epsl.2010.03.017

32. R. Moucha *et al*., Deep mantle forces and the uplift of the Colorado Plateau. *Geophys. Res. Lett.* **36**, L19310 (2009). doi:10.1029/2009GL039778

33. N. A. Simmons, A. M. Forte, S. P. Grand, Thermochemical structure and dynamics of the African superplume. *Geophys. Res. Lett.* **34**, 5 (2007). doi:10.1029/2006GL028009

34. N. A. Simmons, A. M. Forte, S. P. Grand, Joint seismic, geodynamic and mineral physical constraints on three-dimensional mantle heterogeneity: Implications for the relative importance of thermal versus compositional heterogeneity. *Geophys. J. Int.* **177**, 1284 (2009). doi:10.1111/j.1365-246X.2009.04133.x

35. A. M. Forte, in *Treatise on Geophysics*, G. Schubert, Ed. (Elsevier, Amsterdam, 2007), pp. 805-858.

36. L. W. Ward, R. H. Bailey, J. G. Carter, in *The Geology of the Carolinas: Carolina Geological Society anniversary volume*, J. W. Horton, Jr., V. A. Zullo, Eds. (1991), pp. 274-289.

37. B. Haq, A. Al-Qahtani, Phanerozoic cycles of sea-level change on the Arabian Platform. *Geoarabia* **10**, 127 (2005).

38. S. D. Stanford, G. M. Ashley, G. J. Brenner, Late Cenozoic fluvial stratigraphy of the New Jersey Piedmont: A record of glacioeustasy, planation, and incision on a low-relief passive margin. *J. Geol.* **109**, 265 (2001). doi:10.1086/319242

39. R. Oaks, N. Coch, J. Sanders, R. Flint, (Utah State Univ. Press, Logan, Utah, 1974), pp. 53-87.

40. R. Oaks, J. DuBar, *Post-Miocene Stratigraphy, Central and Southern Atlantic Coastal Plain* (Utah State Univ. Press, Logan, Utah, 1974), pp. 232–245.

41. M. E. Raymo, L. E. Lisiecki, K. H. Nisancioglu, Plio-Pleistocene ice volume, Antarctic climate, and the global δ18O record. *Science* **313**, 492 (2006). doi:10.1126/science.1123296 Medline

42. J. J. Groot, R. R. Jordan, *The Pliocene and Quaternary Deposits of Delaware: Palynology, Ages, and Paleoenvironments*. D. G. Survey, Ed., (Delaware Geological Survey, Report of Investigations, 1999), vol. 58, pp. 36.

43. F. Pazzaglia, M. Brandon, Macrogeomorphic evolution of the post-Triassic Appalachian mountains determined by deconvolution of the offshore basin sedimentary record. *Basin Res.* **8**, 255 (1996). doi:10.1046/j.1365-2117.1996.00274.x

44. D. Granger, J. Kirchner, R. Finkel, Spatially averaged long-term erosion rates measured from in situ-produced cosmogenic nuclides in alluvial sediment. *J. Geol.* **104**, 249 (1996). doi:10.1086/629823

45. A. Matmon *et al.*, Temporally and spatially uniform rates of erosion in the southern Appalachian Great Smoky Mountains. *Geology* **31**, 155 (2003). doi:10.1130/0091-7613(2003)031<0155:TASURO>2.0.CO;2

46. A. Matmon *et al.*, Erosion of an ancient mountain range, the Great Smoky Mountains, North Carolina and Tennessee. *Am. J. Sci.* **303**, 817 (2003). doi:10.2475/ajs.303.9.817

47. M. Hulver, Dissertation, The University of Chicago (1997).